# Fiske modes in 0-$\pi$ Josephson junctions

C. Nappi and E. Sarnelli
*Istituto di Cibernetica "E. Caianiello" del CNR, I-80078, Pozzuoli, Napoli, Italy*

M. Adamo
*Dipartimento Scienze Fisiche, Universitá di Napoli "Federico II," Napoli, Italy*
*and Istituto di Cibernetica "E. Caianiello" del CNR, I-80078, Pozzuoli, Napoli, Italy*

M. A. Navacerrada
*Departamento de Física e Instalaciones, Escuela Técnica Superior de Arquitectura, Universidad Politécnica, Avda. Juan de Herrera 4, 28040 Madrid, Spain*

(Received 19 May 2006; published 5 October 2006)

We analyze the influence of an unconventional symmetry order parameter on the dynamical properties of the interface in a grain boundary bicrystal Josephson junction. The self-resonance modes, known as Fiske steps, are calculated by assuming the presence of an arbitrary number of 0-$\pi$ singularities in the phase difference between the two superconducting films. Simple expressions are obtained useful to fit experimental data.

DOI: 10.1103/PhysRevB.74.144504 PACS number(s): 74.50.+r, 85.25.Cp, 61.72.Mm

## I. INTRODUCTION AND BACKGROUND

It is now well established that the properties of $YBa_2Cu_3O_{7-\delta}$ (YBCO) grain boundary Josephson junctions (GBJJ) in films depend on the presence of "facets," 50–100 nm long, in the border with a variety of orientations.[1] The *d*-wave symmetry of the order parameter coupled with the latter circumstance results in a critical current density $J_1$ whose value differs discontinuously, possibly also in sign, from one facet to another. In such cases, the static dependence of the critical current on the external magnetic field becomes highly anomalous.[2] Moreover, in some special cases, as for istance in [001] tilt 0°–45° GBJJs the critical current density is alternating in sign from one facet to the next. Its influence on the magnetic field dependence of the junction critical current $I_c(H)$ was observed by Hilgenkamp *et al.*,[3] Smilde *et al.*[4] and then it was theoretically analyzed by Mints and Kogan.[5]

So far, attention has been mainly dedicated to static properties of high temperature GBJJs, characterizing this type of interface and how the symmetry of the order parameter has an influence on them. Dynamical aspects have been also considered specifically by Chesca[6] and Chesca and Kleiner[7] in the case of SQUIDs (superconducting quantum interference device) made by two GBJJ or in connection with nonlinear propagation in long junctions by Goldobin *et al.*[8] Chesca *et al.* also gave earlier experimental evidence that unconventional superconductivity puts its signature on the Josephson dynamics.[9]

More generally, the effects of an unconventional symmetry of the order parameter on the Josephson effect and the rich variety of implications connected with them have been now the subject of several review papers which give quite a complete perspective on the argument.[10–13]

In this paper we carry out a derivation of the self-resonances occurring in the current-voltage characteristic of a Josephson junction in which the critical current density is a discontinous, changing sign, function of the position along the boundary line. It is well known that some of the structures, or "steps," appearing in the (*I-V*) characteristics of HTS GBJJs have been identified as Fiske resonances.[14] Although the conventional theory of Fiske steps,[15] derived for junctions with uniform current density, has been successfully used for a restricted class of HTS junctions,[14] a specific theory of Fiske steps in HTS GBJJs, accounting for the main peculiarity of this junction, i.e., presence of faceting and a predominantly "*d*-wave" order parameter symmetry, is lacking. Here we derive the dependence on the magnetic field of the maximum amplitude of the *n*th self-resonance in a GBJJ. We base our analysis on the choice of a simple invariant gauge phase difference between the two superconductors, inglobing both a number of 0-$\pi$ discontinuities, regularly or randomly distributed, and the effect of a uniform external magnetic field. In so doing we assume that the elementary two facet 0-$\pi$ junctions present in the GBJJ have a size much smaller than the local Josephson penetration depth so that the magnetic flux induced by the discontinuity can be ignored.

In such considered regime of "flat phase state," i.e., one in which no *spontaneous* flux is allowed, by using a perturbative scheme, we calculate the phase dynamics and the resulting resonances appearing in the current voltage characteristic of a finite length junction. We also predict some characteristic behaviors expected in the experiments and give simple expressions useful to fit experimental data. The paper is organized as follows. In Sec. II we establish the base of our model theory. In Sec. III the calculations leading to the expressions for the Fiske step amplitudes are presented. Section IV uses the results to predict the resonance behaviors in the case of few and many 0-$\pi$ singularities, respectively. Section V draws briefly the conclusions.

## II. JOSEPHSON JUNCTIONS WITH 0-$\pi$ DISCONTINUITIES

### A. Discontinuities in the phase difference

As stated in the preceding section, properties of HTS Josephson junctions are influenced by *d*-wave symmetry of the

 

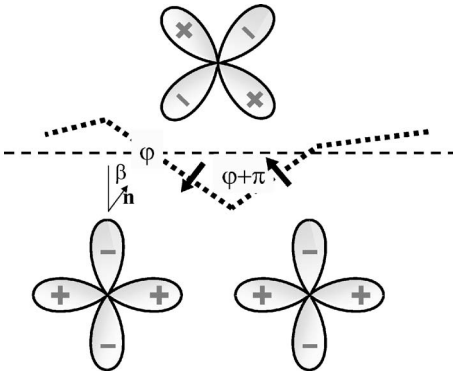


FIG. 1. Schematic drawing of the meandering interface in 0°–45° GBJJ. The $d_{x^2-y^2}$ symmetry of the order parameter, coupled with the varying orientation of the interface, causes the formation of $\pi$-facets. Arrows indicate the direction of tunneling.

order parameter. One of the main consequences is the possibility of 0-$\pi$ discontinuities in the phase difference along the junction. These are obtained either artificially, by appropriate junction fabrication techniques, or because of the intrinsic random mechanism of growth of the junction interface. In the former case, we may indicate artificial superconducting (ferromagnetic) superconductor (SFS) junctions,[17] or YBCO/Au/Nb ramp-edge junctions.[18] In this latter case we find GBJJs techniques, obtained by using both bicrystal[19] or biepitaxial methods.[20] The theory that we have developed may be applied to both cases. For GBJJs a degree of randomicity has also been included. Indeed, the presence of facets with various orientations with respect to the nominal misorientation angle $\theta$ ($0° < \theta \leqslant 45°$), makes GBJJs the place where a random presence of 0-$\pi$ discontinuities may be found, especially for high values of $\theta$. In this work the underlying physics is derived considering the real interface orientation, either artificially made or due to microscopic random oriented facets. The nominal misorientation angle only describes the relative orientations in the two electrodes forming the junction.

As stated above, the possibility of 0-$\pi$ discontinuities in the phase difference is related to the *d*-wave symmetry of pairing wave function in HTS Josephson junctions coupled with the complex structure of their interface. This is characterized by "facets" variously rotated with respect to the misorientation angle, e.g., 0°–45° and across which the current transport takes place. The critical current density strongly depends on this local orientation. When the misorientation angle is sufficiently high the *d*-wave symmetry permits the existence of 0-$\pi$ adjacent facets (see Fig. 1). Here the critical current density has a sign inversion, positive/negative, in going from "0" facet to the "$\pi$" one. The sign inversion mechanism is illustrated in Fig. 1: the phase sign difference of facing lobes of the $d_{x^2-y^2}$-wave order parameter causes $\pi$ local jumps of the phase difference across the junction, which for the Josephson current $j=J_1 \sin(\pi+\varphi)$ is equivalent to a negative $J_1$. The most noteworthy case, from this point of view, is the asymmetric 0°–45° [001] tilt grain boundary in which the alternate orientation of the faceting produces a regular alternating sign of the tunnelling current density when many facets are present. Remarkably this natural mechanism of "phase jump" can be also reproduced in ordinary *s*-wave material junctions, by applying a strongly localized magnetic field (a "$\delta$ Dirac" field) in a chosen point of the junction barrier, by using a localized current injection.[8] The intensity of the current can be regulated so that the local bending of the phase obtained mimics a 0-$\pi$ phase jump.

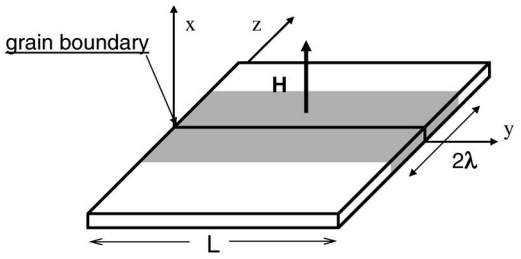


FIG. 2. Schematic drawing of a short YBCO bicrystal GBJJ and coordinate system.

### B. The phase in the presence of 0-$\pi$ discontinuities and magnetic field

In this section, we derive the expressions for the junction phase difference and the magnetic field in the presence of 0-$\pi$ discontinuities. As shown hereafter, such quantities are substantially affected by the presence of discontinuities and their analytical expressions are modified. In this paper we analyze specifically the case 0°–45° [001] tilt grain boundary. We will refer to the system depicted in Fig. 2: a planar junction between two superconducting films asymmetrically rotated by 45° of each other. The grain boundary line is along the *y* coordinate. The gradient of the total phase difference $\mu$ and the magnetic field $H$ in the junction are related by

$$\frac{d\mu}{dy} = \frac{2\pi d_{\text{eff}}\mu_0}{\Phi_0} H(y), \tag{1}$$

where $d_{\text{eff}} \approx 2\lambda$ is the effective junction magnetic penetration depth and $\lambda$ is the London length. In Eq. (1) we will take $H$ as the assigned externally applied magnetic field $H_e$. We also assume that the total length $L$ of the junction is the sum of a number of facets whose length is smaller than the typical local Josephson penetration depth $\lambda_j=(\Phi_0/2\pi\mu_0 J_1 2\lambda)^{1/2}$. In this limit the spontaneous flux generated by a 0-$\pi$ discontinuity is vanishingly small,[21] or even absent,[22] while the external magnetic field fully penetrates the junction so that the *static* phase can be written as

$$\mu(y) = \pi \sum_{k=1}^{N_s} \sigma_k \theta(y - L_k) + \frac{2\pi d_{\text{eff}}\mu_0 H_e}{\Phi_0} y + \psi \tag{2}$$

which accounts for the presence of $N_s$ 0-$\pi$ discontinuities. $\theta(y)$ is the Heaviside unit step function, $L_i$ the location, on the *y* coordinate, of the *i*th 0-$\pi$ discontinuity, $\psi$ an arbitrary constant phase and $\sigma_k = \pm 1$. Thus in the presence of an external uniform magnetic field $H_e$, the phase is uniformly tilted besides displaying an arbitrary number $N_s$ of $\pm\pi$ jumps (see Fig. 3). Introducing $\Theta(y) = \pi \Sigma_{k=1}^{N_s} \sigma_k \theta(y - L_k)$ and $k = 2\pi d_{\text{eff}}\mu_0 H_e/\Phi_0$ we can write Eq. (2) concisely as

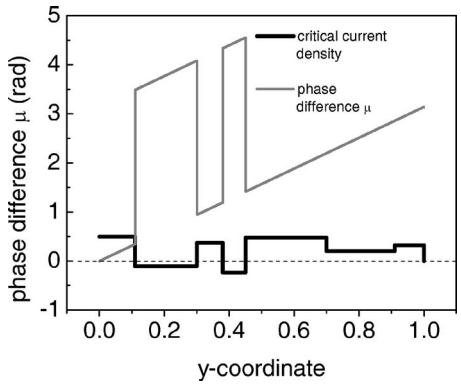


FIG. 3. Representation of the static phase difference $\mu(y)$ (gray) corresponding to the critical current density (black) along the grain boundary line. An inversion point of the critical current density is signaled by a 0-$\pi$ phase-jump discontinuity.

$$\mu(y) = \Theta(y) + ky + \psi. \tag{3}$$

Following this approach we are neglecting any influence of the meandering of the facets on the electromagnetic propagation along the junction and, as far as this aspect is concerned, we consider either an effective propagation direction along the $y$ coordinate or, at most, in the case of few facets, a propagation along the faceting line, a curvilinear coordinate, which ignores "corners." From this point of view the length $L$ of the junction should be interpreted as an effective length. Hence we retain, as the main effect, the influence of the facet meandering is the determination of a discontinuous Josephson critical current density distribution.

It is interesting to observe that the magnetic field associated to a discontinuous phase jump of magnitude $\pi$ at $y = y_0$ and from which the phase jump itself can be thought to be generated, can be represented as a delta function,

$$H_\pi = \pm \frac{\Phi_0}{2d_{\text{eff}}\mu_0}\delta(y - y_0). \tag{4}$$

More in general, in the case of $N_s$ 0-$\pi$ singularities we formally write

$$\frac{d\Theta(y)}{dy} = \pi\sum_{k=1}^{N_s} \sigma_k \delta(y - L_k) \tag{5}$$

so that the singular part of the field, which however does not contribute to the magnetic flux, is

$$H_\pi = \frac{\Phi_0}{2\pi d_{\text{eff}}\mu_0}\frac{d\Theta(y)}{dy} \tag{6}$$

from which Eq. (2) can formally be derived.

### C. The Josephson current density

Also the Josephson current density $J$ is substantially modified because of the presence of nonconventional order parameter symmetry. Indeed, any relative orientation of the $d$-wave lobes associated to the crystal lattice of the electrodes induces in turn a change in $J$.[23] Considering the standard definition of $J$, the Josephson current density takes the form

$$\begin{aligned} J &= J_1 \sin[\Theta(y) + ky + \psi] \\ &= J_1 \sin[\Theta(y)]\cos(ky + \psi) + J_1 \cos[\Theta(y)]\sin(ky + \psi) \end{aligned} \tag{7}$$

with $J_1$ the maximum Josephson current density. Equation (7) implies $J = \pm J_1 \sin(ky + \varphi_0)$, i.e., a sign inversion in $J_1$ occurring at each 0-$\pi$ discontinuity position $L_k$.

Apart from its sign inversions, $J_1$ is in general a function of the $y$ coordinate. Indeed, $J_1(y)$ will assume a constant value in each of the $N$ intervals corresponding to the $N$ facets with alternating orientations forming the grain boundary. Thus $J_1(y)$ is a random discontinuous function, taking constant values (positive or negative), in the $i$th facet $l_i = y_i - y_{i-1}$ along the junction length. We can write $J_1(y)$ as

$$J_1(y) = \begin{cases} j_1, & y_0 < y < y_1, \\ j_2, & y_1 < y < y_2, \\ \cdots, & \\ j_i, & y_{i-1} < y < y_i, \\ \cdots, & \\ j_N, & y_{N-1} < y < y_N. \end{cases} \tag{8}$$

In Eq. (8) $y_0 = 0$, $y_N = L$ and the amplitudes of the $j_i$, in the interval $[y_{i-1}, y_i]$, of size $l_i = y_i - y_{i-1}$, $i = 1, \ldots, N$, are all determined by the orientation of the facets. In this way the number of discontinuities $N_s$ is at most $N-1$. They are obtained directly by the microscopic structure (length and orientation of the single facet) and are related to the order parameter symmetry through the Sigrist-Rice expression.[23] In the case referred in the present paper, that of a 0°–45° tilt asymmetric [001] GBJJ, $j_i$ (amplitude and sign) is given by

$$\begin{aligned} j_i = J_0[\cos^2(\beta_i) - \sin^2(\beta_i)]\Bigg[\cos^2\left(\beta_i - \frac{\pi}{4}\right) \\ - \sin^2\left(\beta_i - \frac{\pi}{4}\right)\Bigg], \end{aligned} \tag{9}$$

where $\beta_i$ is the angle between the interface normal of the $i$th facet and the crystallographic axis (Fig. 1). In what follows we will almost invariably preserve the information on the sign inversion points of $J_1$, e.g., the positions $L_k$'s, by keeping the function $\Theta(y)$ in the argument of the sine in Eq. (7). In this case the $j_i$'s in Eq. (8) or (9) are taken in absolute value.

An important quantity is the average maximum Josephson current density $\langle J_1 \rangle = 1/L\int_0^L |J_1(y)|$. In the present case $J_1(y)$ is a steplike function of $y$ and $\langle J_1 \rangle$ writes

$$\langle J_1 \rangle = \frac{1}{L}\sum_{i=1}^{N} |j_i| l_i, \tag{10}$$

where $\Sigma_{i=1}^N l_i = L$. Then it is also convenient to introduce the effective Josephson penetration depth $\langle \lambda_j \rangle$,

$$\langle \lambda_j \rangle^2 = \frac{\Phi_0}{(2\pi\mu_0 \langle J_1 \rangle 2\lambda)}. \tag{11}$$

Finally, also of interest, for a proper normalization of the current, is $\langle J_1^* \rangle = 1/L \int_0^L J_1(y)$, which in the discrete case, reduces to

$$\langle J_1^* \rangle = \frac{1}{L} \sum_{i=1}^{N} j_i l_i. \tag{12}$$

### D. The magnetic field dependence of the critical current

As stated above we assume short facet junctions, i.e., $l_i \ll \lambda_j^{(i)}$ with $\lambda_j^{(i)} = (\Phi_0/2\pi\mu_0 j_i 2\lambda)^{1/2}$. Then the critical current of a junction of length $L$ can be written as

$$\frac{I_c(H)}{I_1} = \max\left( \frac{1}{LI_1} \int_0^L |J_1(y)| \sin(\Theta(y) + ky + \psi) dy \right), \tag{13}$$

where $I_1 = \langle J_1 \rangle L$, to be distinguished from $I_c(0) = \langle J_1^* \rangle L$, the critical current in zero field, and the maximum value is obtained by varying $0 < \psi < 2\pi$ for each value of $H_e$. It is easily seen that it can be represented by

$$\frac{I_c(H)}{I_1} = \sqrt{A^2 + B^2},$$

$$A = \frac{1}{L} \sum_{i=1}^{N} \frac{|j_1|}{\langle J_1 \rangle} \int_{y_{i-1}}^{y_i} \sin(\Theta(y) + ky) dy,$$

$$B = \frac{1}{L} \sum_{i=1}^{N} \frac{|j_1|}{\langle J_1 \rangle} \int_{y_{i-1}}^{y_i} \cos(\Theta(y) + ky) dy. \tag{14}$$

This expression reduces to that obtained in Ref. 5 when the critical current density alternates between only two values $\mp \bar{j}$ all along the many facets of the grain boundary and to $I_c/I_1 = \sin^2(\pi\Phi/2\Phi_0)/|\pi\Phi/2\Phi_0|$ for the symmetric 0-$\pi$ junction,[24] where $2\pi\Phi/\Phi_0 = kL$ is the total magnetic flux, respectively. An anomalous dependence of the critical current on the external magnetic field is the typical result of the presence of one, or many, 0-$\pi$ junctions (see Fig. 8).

## III. THEORY

In the presence of a steady voltage $V_0$ between the electrodes, the phase difference $\varphi$ increases with time as $2\pi V_0 t/\Phi_0$ and the current oscillates with the Josephson frequency $\omega = 2\pi V_0/\Phi_0$. The Josephson current density, at finite voltages $V_0$, has the form of an exciting wave propagating along the $y$ direction (see Fig. 2). Standing electromagnetic wave modes can build up between 0 and $L$ as in a plane resonator. Within the Kulik[15] (and Eck, Scalapino, and Taylor[16]) theoretical explanation of Fiske steps the Josephson junction simultaneously experiences a steady magnetic field and a steady potential difference. The origin of Fiske steps observed in the current-voltage characteristic of a conventional Josephson junction is ascribed to the ac Josephson effect cavity mode interaction. Standing wave modes of electromagnetic radiation can be determined in GBJJs if the grain boundary is seen as a plate resonator, where the junction barrier forms the effective dielectric medium and the two interconnecting grains the resonator walls, respectively. In the specific case of [001] tilt 45° asymmetric GBJJ a regular faceting causes the maximum Josephson current density $J_1$ to alternate sign along the $y$ direction. The case of nonuniform (but continuous) maximum Josephson current distribution was studied in Ref. 25. Hereafter, retracing that analysis, we mainly specialize to the case of a nonuniform discrete inverting sign distribution and show that neither sign changes nor discontinuities introduce particular difficulties in the new derivation. In the following, for the sake of clarity, we will separate the continuous part of the Josephson phase, $\varphi(y,t)$, from the discontinous one. The relevant equation for $\varphi(y,t)$, takes the form

$$\frac{\partial^2 \varphi}{\partial y^2} - \frac{1}{\bar{c}^2} \frac{\partial^2 \varphi}{\partial t^2} - \frac{\gamma}{\bar{c}^2} \frac{\partial \varphi}{\partial t} = \frac{|J_1(y)|}{\langle J_1 \rangle \langle \lambda_j \rangle^2} \sin[\Theta(y) + \varphi] - \frac{j_{\text{bias}}}{\langle J_1 \rangle \langle \lambda_j \rangle^2}, \tag{15}$$

where $\bar{c}$ is the Swihart velocity and $\gamma$ the quasiparticle tunnell loss coefficient. The phase $\varphi(y,t)$ can be obtained by solving Eq. (15) under the boundary conditions[26]

$$\left. \frac{\partial \varphi}{\partial y} \right|_0 = \left. \frac{\partial \varphi}{\partial y} \right|_L = -\frac{2\pi d_{\text{eff}} \mu_0}{\Phi_0} H_e. \tag{16}$$

The junction current-voltage characteristics can be in turn derived starting from $J = J_1 \sin \mu(y,t)$, where $\mu(y,t) = \Theta(y) + \varphi(y,t)$ is the overall phase difference.

In the limit of low-$Q$ junctions, where $Q$ indicates the quality factor, the Kulik approximation consists of writing the unknown part of the phase $\varphi$ as a sum of two terms $\varphi = \varphi_0 + \varphi_1$ where $\varphi_1 \ll \varphi_0$ and $v = \Phi_0/2\pi d\varphi_1/dt$ is the perturbation to the steady voltage $V_0$,

$$\varphi(y,t) = \varphi_0(y,t) + \varphi_1(y,t) = \omega t - ky + \varphi_1(y,t). \tag{17}$$

To the first order we obtain

$$\frac{\partial^2 \varphi_1}{\partial y^2} - \frac{1}{\bar{c}^2} \frac{\partial^2 \varphi_1}{\partial t^2} - \frac{\gamma}{\bar{c}^2} \frac{\partial \varphi_1}{\partial t} \approx \frac{|J_1(l_i)|}{\langle J_1 \rangle \langle \lambda_j \rangle^2} \sin[\Theta(y) + \omega t - ky], \tag{18}$$

where the perturbation term $\varphi_1(y,t)$ in the argument of sine, on the right-hand side, has been neglected. The boundary conditions (16) for $\varphi_1(y,t)$ complements equation (18),

$$\left. \frac{\partial \varphi_1}{\partial y} \right|_0 = \left. \frac{\partial \varphi_1}{\partial y} \right|_L = 0. \tag{19}$$

In this case, following a standard procedure,[15] we seek $\varphi_1(y,t)$ in the form

$$\varphi_1(y,t) = \sum_{n=0}^{\infty} a_n \cos\frac{n\pi y}{L}\cos\omega t + \sum_{n=0}^{\infty} b_n \cos\frac{n\pi y}{L}\sin\omega t. \tag{20}$$

The coefficients are straightforward obtained by substituting Eq. (20) in Eq. (18). They are given by

$$a_n = -\frac{\bar{c}^2}{\omega^2\langle j_c\rangle\langle\lambda_j\rangle^2}\frac{\left[\left(1-\frac{\omega_n^2}{\omega^2}\right)B_n - \frac{1}{Q}C_n\right]}{\left[\left(1-\frac{\omega_n^2}{\omega^2}\right)+\frac{1}{Q^2}\right]}, \tag{21}$$

$$b_n = \frac{\bar{c}^2}{\omega^2\langle j_c\rangle\langle\lambda_j\rangle^2}\frac{\left[\left(1-\frac{\omega_n^2}{\omega^2}\right)C_n + \frac{1}{Q}B_n\right]}{\left[\left(1-\frac{\omega_n^2}{\omega^2}\right)+\frac{1}{Q^2}\right]}, \tag{22}$$

where

$$B_n = \frac{2}{L}\sum_{i=1}^{N}\frac{|j_i|}{\langle J_1\rangle}\int_{y_{i-1}}^{y_i}\sin[ky-\Theta(y)]\cos\frac{n\pi y}{L}dy, \tag{23}$$

$$C_n = \frac{2}{L}\sum_{i=1}^{N}\frac{|j_i|}{\langle J_1\rangle}\int_{y_{i-1}}^{y_i}\cos[ky-\Theta(y)]\cos\frac{n\pi y}{L}dy. \tag{24}$$

The net Josephson current is given by $J=J_1\sin[\Theta(y)+\varphi_0+\varphi_1]$. This is frequency modulated and contains a nonzero dc term which can be extracted by a time, $\langle\cdots\rangle$, and space, $\frac{1}{L}\int_0^L\cdots dy$, average procedure, $J_{\rm dc}\approx\frac{1}{L}\int_0^L J_1\langle\varphi_1\cos[\Theta(y)+\omega t-ky]\rangle dy$. The result is

$$J_{\rm dc} = \frac{\bar{c}^2\langle J_1\rangle}{4\omega^2\langle\lambda_j\rangle^2}\sum_{n=1}^{\infty}\frac{1/Q_n}{1/Q_n^2+(1-\omega_n^2/\omega^2)^2}(B_n^2+C_n^2). \tag{25}$$

We define $F_n^2(\phi)=B_n^2+C_n^2$ and calculate the maximum amplitude ($\omega=\omega_n=n\pi\bar{c}/L$) of the $n$th step as

$$J_n^M(\phi) = \frac{\langle J_1\rangle L^2}{4\langle\lambda_j\rangle^2}\frac{Q_n}{n^2\pi^2}F_n^2(\phi). \tag{26}$$

We explicitly note that the voltage positions $V_n=(\Phi_0/2\pi)\omega_n$, at which the resonances appear, are the same of those expected in a conventional junction of the same length and are by no means affected, in the present approximation, by the modifications introduced to account for the presence of 0-$\pi$ singularities. Also we note that the result obtained, Eqs. (23)–(26), consists of substituting the critical current density Eq. (8) in the final result of the conventional case. On the contrary, the presence of Fiske steps in the absence of an external magnetic field, as well as their amplitude modulation in magnetic field are radically modified by the existance of 0-$\pi$ discontinuities as predicted by Eq. (26).

Finally it is interesting to note that the magnetic behaviors predicted by Eq. (26), in the case in which the singularities are equally spaced (see Figs. 4, 5, and 9), coincide, as can be easily shown, with those predicted by Eq. (2) of Ref. 7 which was derived for a SQUID made of two GBJJ. This is obtained in the limit in which the "system" SQUID reduces, as far as resonances are concerned, to only one junction ($n_1=0$ or $n_2=0$ in the notation of Ref. 7). However all remaining cases of irregularly spaced singularities fall exclusively in the domain of Eqs. (23)–(26).

## IV. RESULTS AND DISCUSSION

### A. Few singularities

In this section we study the self-resonance modes of a GBJJ containing one (or two singularities). This case is an important point of reference useful both to familiarize with the results and in view of possible experiments on submicron GBJJ[27] or on low $T_c$ small junctions with injected current. In the latter case possible deviations from the dependencies hereafter illustrated is a new probe of the influence of the spontaneous flux influence.

#### *1. Self-resonant modes in a junction with one 0-$\pi$ singularity*

We begin to illustrate the results, Eq. (25), by considering the case of a two-facet junction, with a single 0-$\pi$ discontinuity positioned at $L_1$, characterized by two current densities $|j_1|$ and $|j_2|$, respectively. In this case the amplitude of the $n$th function $F_n^2(\phi)$ depends on the following analytical expressions for $B_n$ and $C_n$, respectively,

$$B_n = \frac{2}{k^2L^2-n^2\pi^2}\left(\frac{|j_1|}{\langle J_1\rangle}kL + \frac{|j_2|}{\langle J_1\rangle}kL\cos kL\cos n\pi - \frac{|j_1|+|j_2|}{\langle J_1\rangle}kL\cos\frac{L_1}{L}n\pi\cos kL_1 - \frac{|j_1|+|j_2|}{\langle J_1\rangle}n\pi\sin kL_1\sin\frac{L_1}{L}n\pi\right), \tag{27}$$

$$C_n = \frac{2}{k^2L^2-n^2\pi^2}\left(-\frac{|j_2|}{\langle J_1\rangle}kL\sin kL\cos n\pi + \frac{|j_1|+|j_2|}{\langle J_1\rangle}kL\cos\frac{L_1}{L}n\pi\sin kL_1 - \frac{|j_1|+|j_2|}{\langle J_1\rangle}n\pi\cos kL_1\sin\frac{L_1}{L}n\pi\right). \tag{28}$$

In particular in zero field, $k=0$,

$$F_n^2(0) = \frac{4\left(\frac{|j_1|+|j_2|}{\langle J_1\rangle}\sin n\pi\frac{L_1}{L}\right)^2}{n^2\pi^2} \tag{29}$$

which shows that in the case of symmetric ($L_1=0.5$) 0-$\pi$ singularity, only odd steps exist in zero external field. Figure 4 shows the function $F_n^2(\phi)/n^2=J_n^M(\phi)/[\langle J_1\rangle L^2Q_n/4\langle\lambda_j\rangle^2\pi^2]$ for $n=1,2,3$ in the case $|j_1|=|j_2|$. The dashed curve illustrates, for $n=1$ and $L_1=0.65$, the effect of a small deviation from the symmetric case. It is worth noting that the ratio between the theoretical amplitude of the third step and the first step (symmetric 0-$\pi$ singularity) at zero field is $[F_3^2(0)/3^2]/[F_1^2(0)/1^2]=0.012$, where we assumed $Q_1\approx Q_3$.

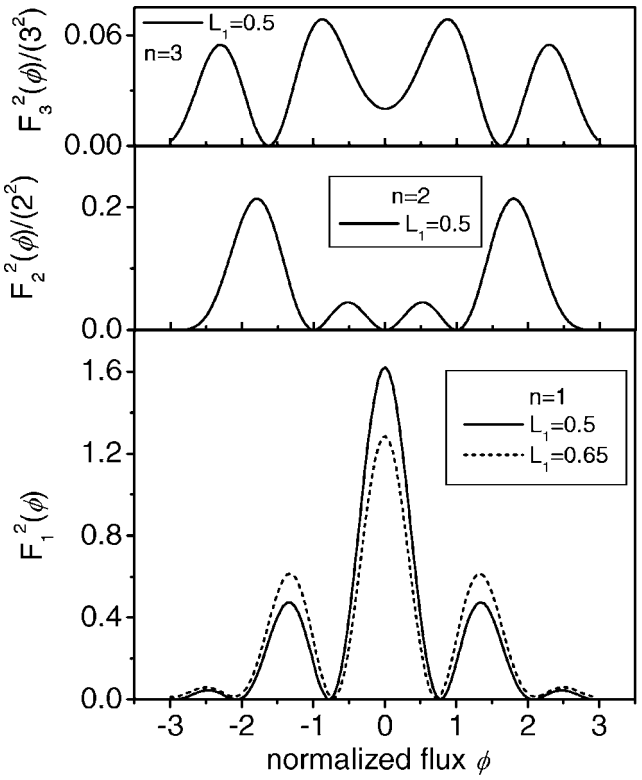


FIG. 4. Theoretical magnetic field dependence of the Fiske steps in a 0-$\pi$ junction. $\frac{F^2(\phi)}{n^2}$ vs $\frac{\Phi}{\Phi_0}$, first three steps, $n=1,2,3$ for $|j_1|=|j_2|$, $L_1/L=0.5$. Dashed line, $L_1/L=0.65$.

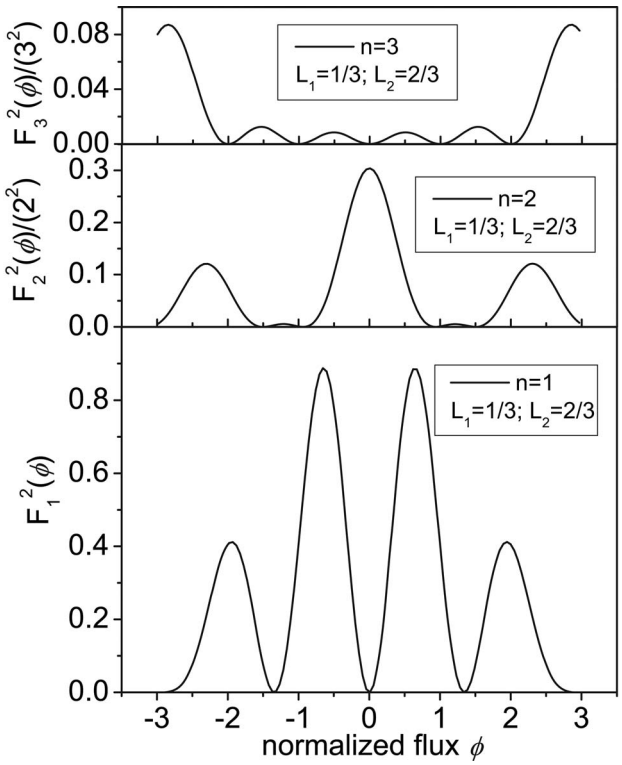


FIG. 5. Theoretical magnetic field dependence of the Fiske steps in a 0-$\pi$-2$\pi$, junction. The phase is discontinuous at $L_1=L/3$, $L_2=2L/3$. $\frac{F^2(\phi)}{n^2}$ vs $\frac{\Phi}{\Phi_0}$, first three steps, $n=1,2,3$.

This means that in a possible experiment with a single 0-$\pi$ junction, aimed to observe resonances in the current voltage characteristic, only the first Fiske step at $V_1=\Phi_0\bar{c}/2L$ should be clearly measurable. Then it is interesting to compare these results with the observations made in Ref. 8. In that experiment, once the conditions of a 0-$\pi$ junction are realized (as shown by the magnetic field critical current pattern) the external magnetic field is turned off ($k=0$) and the current voltage characteristic measured. The single semi-integer ZFS observed under these conditions, at the position $V_1$, has many points of contact with the argumentations here developed. More precisely, it seems quite reasonable that such structure would persist as a resonant current singularity in the current-voltage characteristic, when the size of the junction is made shorter than $\lambda_j$. The spontaneous flux would tend in that case to disappear,[21] and the semi-integer ZFS dynamics simply reduces to the first Fiske step dynamics here described. From this point of view what is essential in that kind of dynamics is the 0-$\pi$ discontinuity rather than the presence of spontaneous flux.

#### *2. Self-resonant modes in two* 0-$\pi$ *singularity junction*

For the sake of further illustration we have calculated the effect of a double 0-$\pi$ singularity (0-$\pi$-0 or, which is the same, 0-$\pi$-2$\pi$) positioned at $L_1$ and $L_2$ so that the junction is divided in three equal size phase zones, $L_1=L/3$, $L_2=2L/3$, or it is divided such that the overall Josephson critical current density is zero, $L_1=L/4$ and $L_2=3L/4$. The sign of $j_1$, $j_2$, $j_3$ being positive, negative, positive, respectively. In these simulations the condition of equal current densities has been chosen for simplicities, i.e., $|j_1|=|j_2|=|j_3|$. The results are shown in Figs. 5 and 6.

### B. Many singularities

In this section we are concerned with the effect caused by the presence of a high number of facets typically encountered in GBJJs at a micrometer scale. First, generalizing Eq. (29), we obtain the maximum amplitude of the Fiske resonances in zero magnetic field in the case of $N$ singularities distributed at $L_1, L_2, \ldots, L_N$,

$$F_n^2(0) = \frac{4}{n^2\pi^2}\left(\sum_{i=1}^{N}(-1)^{i+1}\frac{|j_i|+|j_{i+1}|}{\langle J_1\rangle}\sin\frac{L_i}{L}n\pi\right)^2. \quad (30)$$

From now on we will focus the attention on the case of just two-value alternating critical current density of the type described by Eq. (8), i.e., $J_1=\pm\bar{j}$ in the presence of many facets. To demonstrate the main features of the function $F_n(\phi)$ we first treat the indicative simple case of a continuous sine current density distribution (Fig. 7), then we turn to the case of a discontinuous alternating current introducing also the effect of an increasing degree of disorder (Figs. 9–11). We finally illustrate the effect of a many-facet junction, in which the facets are equal in length and randomly oriented (Fig. 12). The current density amplitude in all such cases is determined through Eqs. (8) and (9).

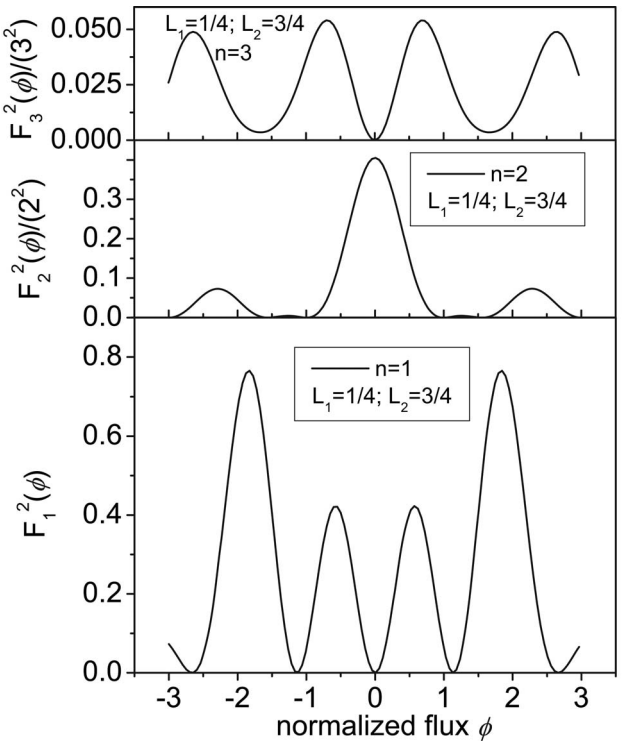


FIG. 6. Theoretical magnetic field dependence of the Fiske steps in a 0-$\pi$-2$\pi$ junction. The phase is discontinuous at $L_1=L/4$, $L_2=3L/4$. $\frac{F^2(\phi)}{n^2}$ vs $\frac{\Phi}{\Phi_0}$, first three steps, $n=1,2,3$.

### 1. Sine periodical distribution of the critical current density

As in Ref. 5 we start by considering the simple periodic sine dependence model

$$J_1(y) = j_0 + j_1 \sin(\pi N y/L) \tag{31}$$

corresponding to a critical current in zero magnetic field $I_c(0)=j_0L$. In Eq. (31), $N$ can still be identified with the number of *facets* with alternating current density between 0 and $L$ as in (8). Figure 7 shows the field dependence of $J_1^M$ for $N=50$ and $j_0=0$ (a), $j_0=0.4j_1$ (b). These values are the same as in Ref. 5. We also show for a quick comparison in Fig. 8 the corresponding result obtained for the $I_c(\phi)$ by Eq. (13) which coincides with the result previously obtained in Ref. 5. The two-lobe structure of the first Fiske step occurs at $\phi=\pm 25$ (one flux quantum for sign inversion). Its position is shifted from the central position $\phi=0$ in the same way as the main peak in the critical current pattern. However, for the nonzero average critical current density [Fig. 7(b)] the current of the first step also displays a standard two-lobe structure[28] at $\phi=0$.

### 2. Discontinuous alternating current density and effect of disorder

Now we illustrate the effect of disorder in the spatial distribution of 0-$\pi$ discontinuities and hence in the spatial distribution of $J_1(y)$ on the field dependence of step current $J_n^M$.

We will consider the self-resonances excited in a junction with alternating critical current density due to the presence of distributed singularities. The critical current density alternates sequentially along $y$ taking two values $j_1$ and $-j_1$, respectively, in $[a_i,b_i]$ and $[b_i,a_{i+1}]$, where $i=1,2,\ldots,N$. Thus $J_1=j_1$ within $N$ intervals with lengths $l_i^+=b_i-a_i$ and $J_1=-j_1$ within $N$ intervals $l_i^-=a_{i+1}-b_i$. In this simplified case the calculation of the $n$th step consists of the evaluation of the coefficients

$$B_n = \frac{2}{L}\sum_{i=1}^{\infty}\left[\int_{a_i}^{b_i}\sin(ky)\cos\frac{n\pi y}{L}dy - \int_{b_i}^{a_{i+1}}\sin(ky)\cos\frac{n\pi y}{L}dy\right], \tag{32}$$

$$C_n = \frac{2}{L}\sum_{i=1}^{\infty}\left[\int_{a_i}^{b_i}\cos(ky)\cos\frac{n\pi y}{L}dy - \int_{b_i}^{a_{i+1}}\cos(ky)\cos\frac{n\pi y}{L}dy\right], \tag{33}$$

We consider a GBJJ such that the facet angle just alternates between two values while the size of the facets is randomly distributed. In this way Eq. (9) gives only two possible values for the current. More precisely, the simulation starts with the generation of a long bicrystal structure, characterized by the presence of random length facets. Then, a bicrystal junction of assigned micrometer length is cut from the long bicrystal. Before disorder is added, the facets have all the same size $\bar{l}$ and their orientation alternates regularly between two fixed angles $\beta$ and $\pi$-$\beta$, such that a zig-zag perfect junction is obtained along the $y$ coordinate [see Fig. 9(a)]. With the choice $\beta=22.5°$ one obtain from Eq. (9) for the maximum value of $\bar{j}$, $J_1=\pm 0.5$. Figure 9(a) shows the "grain boundary," 2 $\mu$m long, each facet $\bar{l}=100$ nm, to which corresponds the current density distribution of Fig. 9(b). Figures 9(c) and 9(d) show the critical current and the first Fiske step maximum amplitude dependence on the magnetic flux, respectively.

Then disorder is added progressively and the effect on the critical current diffraction pattern and the first Fiske step

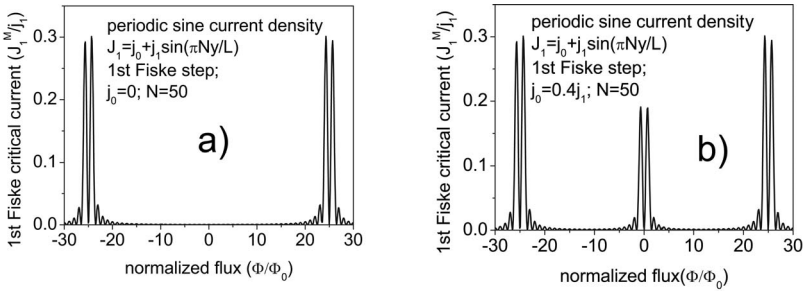


FIG. 7. The dependence of the normalized maximum amplitude of the first Fiske step $J_1^M/j_1$ on $\Phi/\Phi_0$. (a) $j_0=0$. (b) $j_0=0.4j_1$.

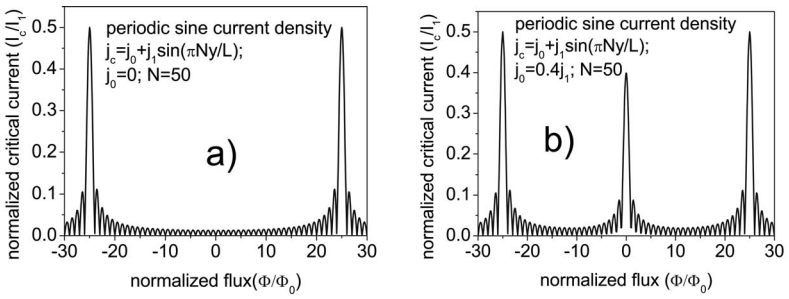


FIG. 8. The dependence of the normalized maximum amplitude of the critical current. $J_1/j_1$ on $\Phi/\Phi_0$. (a) $j_0=0$. (b) $j_0=0.4j_1$.

amplitude dependence on the magnetic field is synthetically illustrated in Figs. 10 and 11. Maintaining the choice $\beta=22.5°$ the length of the facets is considered a random variable *uniformly* distributed in an interval $[a,b]$ centered around $\bar{l}$ so that its mean value is $\bar{l}$ and the variance $\sigma^2=(a-b)^2/12$. In Fig. 10 $a=60$ nm and $b=140$ nm were chosen ($\sigma\simeq 23$ nm). Figures 10(a) and 10(b) show the obtained "grain boundary" with the corresponding current density distribution. Figures 10(c) and 10(d) show the effects on the critical current pattern and the first Fiske amplitude, respectively. Figure 11 corresponds to even higer disorder, with $a=20$ nm and $b=180$ nm ($\sigma\simeq 46.1$ nm). Both the critical current and the Fiske resonance amplitude dependencies are strongly disturbed. Finally, Fig. 12, considers the complementary possibility to add disorder to the facet orientation by keeping a constant length facet. In this case the current density distributions may assume different amplitudes from one interval to another of the same size. The size of the intervals is $\bar{l}=100$ nm while the angle $\beta$ is treated as a random variable uniformly distributed in the interval $[0°,45°]$ around the value $\beta=22.5°$. Figure 12(b) shows the resulting current density distribution calculated through Eq. (9).

## V. CONCLUSIONS

In conclusion, we have developed a theory for describing the magnetic field dependences of Josepshon junctions and Fiske steps in "*d*-wave" grain boundary junctions. In particular, we have extended the theory developed by Kulik in the case of conventional "*s*-wave" superconductors ("0"-type junction) to "0-$\pi$" GBJJs. Our theory can be applied to regular and randomly generated grain boundaries made by "*d*-wave" superconductors. We stress that in the limit $L/\lambda_j\rightarrow 0$ there is no $\pi$ vortex at the 0-$\pi$ discontinuity and no *spontaneous* flux associated. So the magnetic field modulation of the critical current, as well as the resonance amplitude modulations, just reflects the pairing state symmetry and the only flux present is the flux generated by the external magnetic field. We have shown the main features of asymmetric 0°–45° "*d*-wave" grain boundary junctions, with one "0-$\pi$" phase discontinuity. This structure can be made by employing deep submicron GBJJs or artificial low/high-$T_c$ junction technologies as the YBCO/Au/Nb or all low-$T_c$ *S*/*F*/*S* devices. We have addressed the differences that arise when the singularity is in the middle of the junction or in a nonsymmetric position. Also, the effect of facets with both random

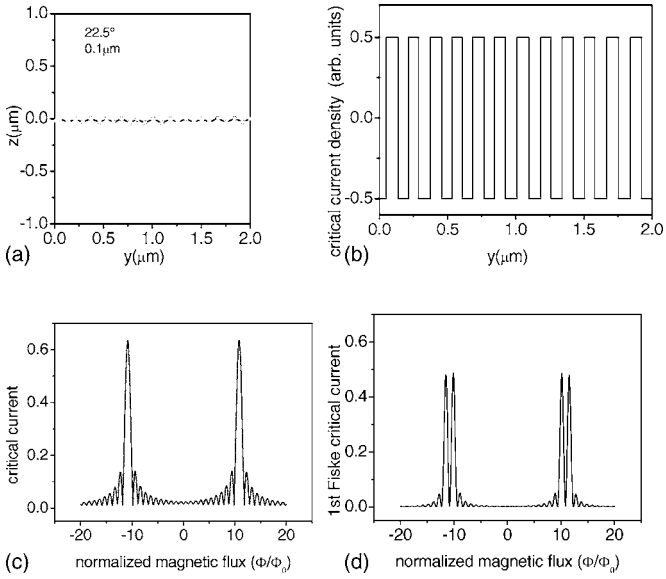


FIG. 9. (a) Simulated meandering with zero variance. (b) Corresponding critical current density. (c) The dependence of the normalized maximum amplitude of the critical current $I_c/I_1$ on $\Phi/\Phi_0$. (d) The dependence of the maximum amplitude of the first Fiske step $J_1^M$ on $\Phi/\Phi_0$.

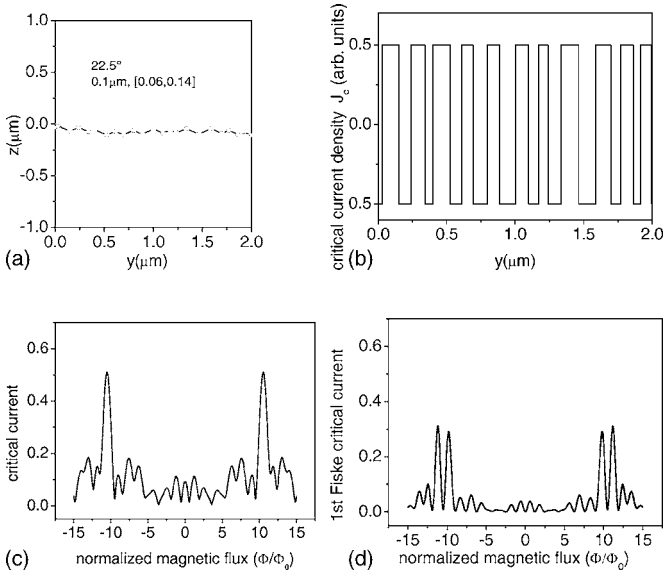


FIG. 10. (a) Simulated meandering ($\sigma=23$ nm). (b) Corresponding critical current density. (c) The dependence of the normalized maximum amplitude of the critical current $I_c/I_1$ on $\Phi/\Phi_0$. (d) The dependence of the maximum amplitude of the first Fiske step $J_1^M$ on $\Phi/\Phi_0$.

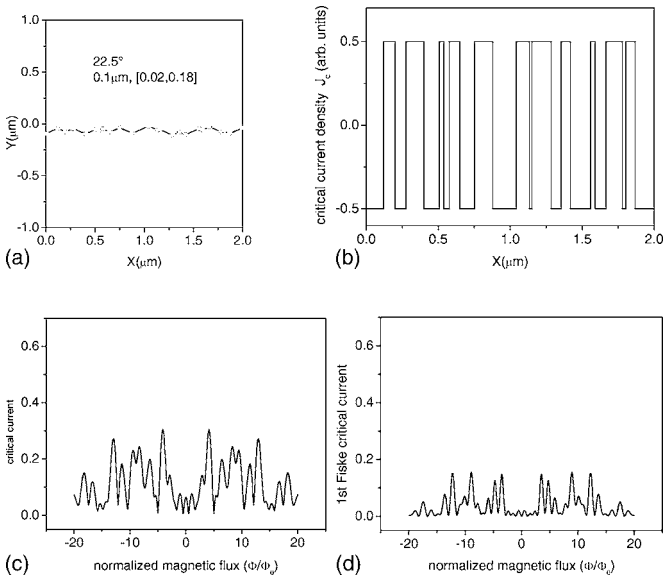


FIG. 11. (a) Simulated meandering ($\sigma$=46.1 nm). (b) Corresponding critical current density. (c) The dependence of the normalized maximum amplitude of the critical current $I_c/I_1$ on $\Phi/\Phi_0$. (d) The dependence of the maximum amplitude of the first Fiske step $J_1^M$ on $\Phi/\Phi_0$.

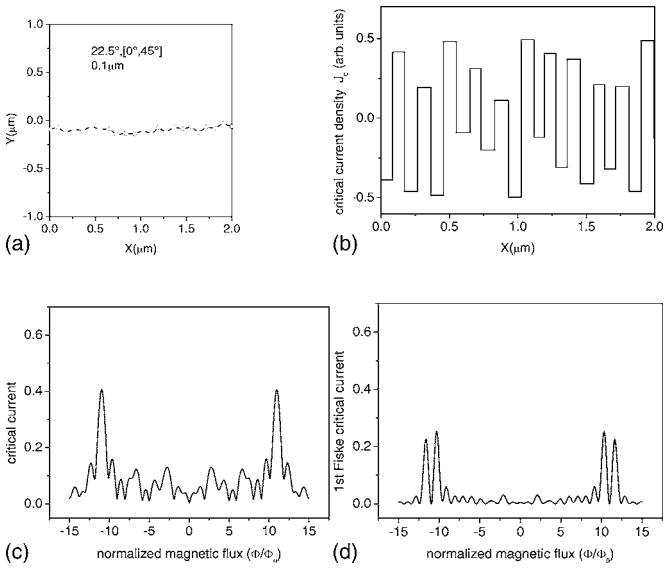


FIG. 12. (a) Simulated meandering with uniformly random ($\sigma_\beta$=12.9°) facet orientation. (b) Corresponding critical current density. (c) The dependence of the normalized maximum amplitude of the critical current $I_c/I_1$ on $\Phi/\Phi_0$. (d) The dependence of the maximum amplitude of the first Fiske step $J_1^M$ on $\Phi/\Phi_0$.

length and orientation has been shown. Moreover considerations on higher order Fiske steps have also been done. Finally, analytical expressions of the amplitude of the magnetic field dependences of Fiske steps in the presence of single symmetric 0-$\pi$ discontinuity and the zero-field Fiske resonances have been derived.

## ACKNOWLEDGMENTS

This work has been partially supported by the ESF Network "Pi-shift," the project DG236RIC "NDA," and the TRN "De-QUACS."

[1] J. Mannhart, H. Hilgenkamp, B. Mayer, Ch. Gerber, J. R. Kirtley, K. A. Moler, and M. Sigrist, Phys. Rev. Lett. **77**, 2782 (1996).
[2] J. Mannhart and H. Hilgenkamp, Physica C **317-318**, 383 (1999).
[3] H. Hilgenkamp, J. Mannhart, and B. Mayer, Phys. Rev. B **53**, 14586 (1996).
[4] H. J. H. Smilde, Ariando, D. H. A. Blank, G. J. Gerritsma, H. Hilgenkamp, and H. Rogalla, Phys. Rev. Lett. **88**, 057004 (2002).
[5] R. G. Mints and V. G. Kogan, Phys. Rev. B **55**, R8682 (1997).
[6] B. Chesca, Ann. Phys. **8**, 511 (1999).
[7] B. Chesca and R. Kleiner, Physica C **350**, 180 (2001).
[8] E. Goldobin, A. Sterck, T. Gaber, D. Koelle, and R. Kleiner, Phys. Rev. Lett. **92**, 057005 (2004).
[9] B. Chesca, R. R. Schulz, B. Goetz, C. W. Schneider, H. Hilgenkamp, and J. Mannhart, Phys. Rev. Lett. **88**, 177003 (2002).
[10] C. C. Tsuei and J. R. Kirtley, Rev. Mod. Phys. **72**, 969 (2000).
[11] A. Barone, J. R. Kirtley, F. Tafuri, and C. C. Tsuei, Phys. Scr., T **T102**, 51 (2002).
[12] F. Tafuri and J. R. Kirtley, Rep. Prog. Phys. **68**, 2573 (2005).
[13] H. Hilgenkamp and J. Mannhart, Rev. Mod. Phys. **74**, 485 (2002).
[14] D. Winkler, Y. M. Zhang, P. A. Nilsson, E. A. Stepantsov, and T. Claeson, Phys. Rev. Lett. **72**, 1260 (1994).
[15] I. O. Kulik, Zh. Eksp. Teor. Fiz. Pis'ma Red. **2**, 134 (1965) [JETP Lett. **2**, 84 (1965)].
[16] R. E. Eck, D. J. Scalapino, and B. N. Taylor, Phys. Rev. Lett. **13**, 15 (1964).
[17] V. V. Ryazanov, V. A. Oboznov, A. Yu. Rusanov, A. V. Veretennikov, A. A. Golubov, and J. Aarts, Phys. Rev. Lett. **86**, 2427 (2001).
[18] H. J. H. Smilde, H. Hilgenkamp, G. J. Gerritsma, D. H. A. Blank, and H. Rogalla, Physica C **350**, 269 (2001).
[19] P. Chaudhari, J. Mannhart, D. Dimos, C. C. Tsuei, J. Chi, M. M. Oprysko, and M. Scheuermann, Phys. Rev. Lett. **60**, 1653 (1988).
[20] A. H. Miklich, J. Clarke, M. S. Colclough, and K. Char, Appl. Phys. Lett. **60**, 1899 (1992).
[21] J. R. Kirtley, K. A. Moler, and D. J. Scalapino, Phys. Rev. B **56**, 886 (1997).
[22] A. Zenchuk and E. Goldobin, Phys. Rev. B **69**, 024515 (2004).
[23] M. Sigrist and T. M. Rice, J. Phys. Soc. Jpn. **61**, 4283 (1992).
[24] D. J. Van Harlingen, Rev. Mod. Phys. **67**, 515 (1995).
[25] M. Russo and R. Vaglio, Phys. Rev. B **17**, 2171 (1978).
[26] These boundary conditions, derived for the present case of "in plane" junctions, are identical to those which apply to the "overlap" junction case.
[27] E. Sarnelli, C. Nappi, M. Adamo, and M. A. Navacerrada, Physica C **437-438**, 274 (2006).
[28] A. Barone and G. Paternó, *Physics and Applications of the Josephson Effect* (Wiley, New York, 1982).